

Observed-based Event-triggered Sliding Mode Control of Networked Control System for Carbon Fiber Diagonal Loom

Xiang Li, Wei Liu and Li Zhang

School of Mechanical Engineering, Tiangong University, Tianjin 300387, China

Abstract

In this paper, an observed-based sliding mode control with event-triggered mechanism for the carbon fiber diagonal loom tension networked control is studied. According to the characteristics of the loom, the networked control is introduced into the loom tension control, the influence of the introduction of network factors is fully considered, and a tension model containing network factors is finally established. An observed-based sliding mode control is adopted. Meanwhile, to further reduce the amount of data transmission and improve the service life of the equipment, an event-triggered condition is also introduced, then the asymptotically stability of the proposed control system and the feasibility of control performance are proved through the Lyapunov functional. Finally, the rapid feasibility of the proposed algorithm is demonstrated by a simulation example.

Keywords

Networked Control; Event-triggered Mechanism; Sliding Mode Control; Tension Control.

1. Introduction

Carbon fiber is a material composed of extremely thin strands of the element carbon with high tensile strength and is extremely durable. It is used to produce carbon fiber reinforced polymer that finds applications in transportation, textile, marine, wind energy, aerospace and defense, construction, consumer goods, and others [1]. In the textile industry, the tension of the yarn is an important quality influence factor when processing carbon fiber fabrics [2]. Too much tension will cause the yarn to break, while too little tension will not roll the yarn into shape.

Recently, lots of advanced control algorithms have been applied to loom tension control. For example, reference [3] proposed an improved genetic algorithm to optimize the PID control scheme, the proposed algorithm overcomes the problem that the control performance of the traditional PID control algorithm in the loom tension control system declines. Reference [4] applied the equivalent sliding mode control on carbon fiber diagonal loom to improve the tension control performance and have good robustness to disturbances. To overcome the shortcoming that the dynamic sliding surface evolution time of discrete global sliding mode control is too long, Reference [5] proposed a fast discrete global sliding mode control method, which not only has strong global robustness, but also can quicken the system response and shorten the transition time. Reference [6] improves the control level of warp tension and the driving performance of the let-off roll system based on fuzzy neural network and vector control. Reference [7] proposed a fuzzy optimal integral separation PID warp tension control scheme based on process sampling to improve the warp tension control level of the loom. Reference [8] proposes an improved model and combines it with genetic algorithms and gradient-based methods to calculate the optimal setting parameters of the weaving process to ensure fabric quality.

However, considering that the loom is a complex distributed mechanical system with multiple control degrees of freedom, its system design contains lots of control units. Also, to realize the

information exchange between the equipment, improve the control accuracy, and reduce the control cost, it is considered to introduce the networked control technology into the tension control of the loom.

A networked control system (NCS) is a control system in which the control loop is closed through a communication network. The defining characteristic of NCS is that the control and feedback signals are exchanged between the system components in packets over the network. Due to the introduction of network factors, problems such as delay, packet loss, quantization, and network attacks also follow [9]. Therefore, it is necessary to additionally consider the influence of network factors on the tension control effect while researching the networked constant tension control of the loom, to improve the quality of the woven fabric.

This paper proposes an observed-based event-triggered sliding mode control method that aims to solve the above problems in discrete-time networked control system with delay, packet loss, and considers the quantization problem in data transmission. The stochastic Lyapunov method is applied to analyze the asymptotic mean-square stability of the proposed control system. The proposed control law can attenuate the effects of the network so that the system state can approach the pre-designed sliding surface in a limited time.

2. Mathematical Modeling of The Loom

The carbon fiber diagonal loom is a complex distributed mechanical system with multiple control degrees of freedom based on carbon fiber materials' high performance. Its system contains plenty of control units and has features such as non-linearity, randomness, and time variety. As shown in Figure 1, yarn is sent from the warp beam, passes through the fixed beam and the tension roller to the heald frame, then across the friction roller and is bundled by the cloth beam.

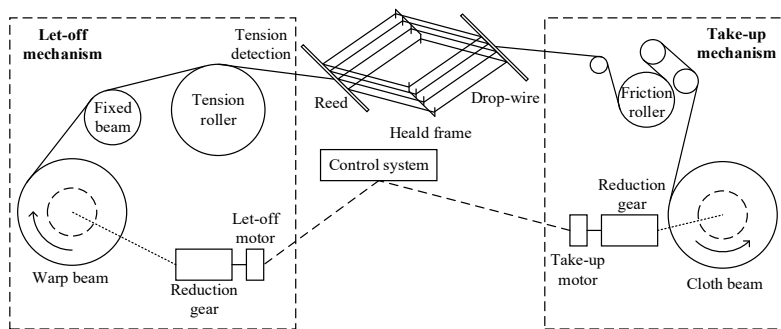


Figure 1. Working principle of the loom

2.1. Friction Modeling

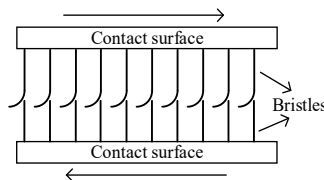


Figure 2. Schematic of the LuGre model

In the process of yarn processing, friction is one of the most important influencing factors. In previous studies, only viscous friction was considered. To improve the accuracy of the proposed tension model, a nonlinear dynamic friction model which named as the LuGre friction model is applied in this paper. The LuGre model derives the roughness between two contacting surfaces at the microscopic scale using elastic bristles, and the dynamic effect of friction results from the average deflection of these bristles. The LuGre model more accurately simultaneously describes

sliding displacement, memory friction, variable static friction, viscous friction and Stribeck curve effects [10].

A LuGre friction mathematical modeling can be described as follow:

$$\begin{cases} \frac{dz}{dt} = \omega - \frac{|\omega|}{g(\omega)} z \\ \sigma_0 g(\omega) = F_c + (F_s - F_c) \exp\left(-\frac{|\omega|}{\omega_s}\right) \\ M_f = \sigma_0 z + \sigma_1 \frac{dz}{dt} + C_s \omega \end{cases} \quad (1)$$

where z is the distance between the contact surfaces where the bristles are offset; ω is the angular velocity of the warp beam; σ_0 , σ_1 and C_s are the stiffness coefficient, damping coefficient, and viscous friction coefficient of the bristles respectively; F_c and F_s are coulombs friction torque and static friction torque, respectively and $F_c > F_s$; ω_s is the Stribeck speed which is a small positive number, and M_f is the total friction torque. According to the values of ω and ω_s , the yarn friction can be divided as viscous friction when $|\omega| < \omega_s$ and sliding friction when $|\omega| > \omega_s$.

According to the friction characteristics, when ω is large, that is, in the pure sliding friction state, $dz/dt \approx 0$; when ω is small and commutated, that is, in the viscous state, there is a large value of $dz/dt \approx 0$. Therefore, for the pure sliding friction state, according to (1), the value of z can be obtained as follow:

$$z = |g(\omega)| \quad (2)$$

According to (1) and (2), in the sliding state, the friction torque based on the LuGre model is as follow:

$$M_f = F_c + (F_s - F_c) \exp\left(-\frac{|\omega|}{\omega_s}\right) + C_s \omega \quad (3)$$

Since ω_s is exceedingly small, then according to the characteristic of the exponential function, Equation (3) can be simplified as follow:

$$M_f = F_c + C_s \quad (4)$$

2.2. Let-off System Modeling

Figure 3 stands for the schematic of the let-off system. The warp beam's radius $r_1(t)$ is decreasing gradually, suppose that the warp beam's maximum radius is R_{1max} each layer of warp yarn has a thickness of δ , and the warp beam rotates $\varphi(t)$ times per minute. So, warp beam's radius $r_1(t)$ is as follow:

$$r_1(t) = R_{1max} - \frac{\varphi(t)}{2\pi} \delta \quad (5)$$

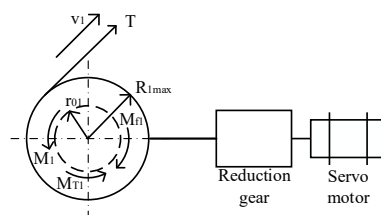


Figure 3. Schematic of let-off system

Since the radius of the warp beam changes with time, its moment of inertia J_1 is also a time-varying value as follow:

$$J_1 = J_{01} + J_{r1} \tag{6}$$

where J_1 stands for the moment of inertia of the warp beam, $J_{r1} = \pi\rho b(R_{1max}^4 - r_{01}^4)/2$ stands for the moment of inertia of the yarn on the warp beam with r_{01} is the initial radius.

Then, Equation (7) can be obtained according to the dynamic balance equation:

$$i_1M_1 + M_{T1} - M_{f1} = J_1 \frac{d\omega_1}{dt} \tag{7}$$

where i_1 stands for reduction ratio of the reduction gear, $M_{T1} = Tr_1$ stands for motor torque with T is the yarn tension, $M_{f1} = F_{c1} + C_{s1}\omega_1$ stands for friction torque, ω_1 stands for the angular velocity of warp beam.

2.3. Take-up System Modeling

Similar to the let-off system, Figure 4 is the schematic of take-up system, and the warp beam's radius is

$$r_2(t) = r_{02} + \frac{\varphi(t)}{2\pi} \delta \tag{8}$$

where r_{02} is the initial radius of the warp beam. The moment of inertia is

$$J_2 = J_{02} + J_{r2} \tag{9}$$

where J_2 stands for the moment of inertia of the warp beam, $J_{r2} = \pi\rho b(R_2^4 - r_{02}^4)/2$ stands for the moment of inertia of the yarn on the warp beam with R_2 and r_{02} are the time-varying radius and the initial radius, respectively.

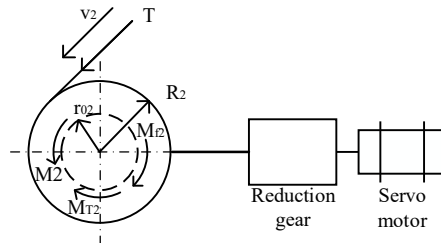


Figure 4. Schematic of take-up system

Then, Equation (10) can be obtained according to the dynamic balance equation:

$$i_2M_2 - M_{T2} - M_{f2} = J_2 \frac{d\omega_2}{dt} \tag{10}$$

where i_2 stands for reduction ratio of the reduction gear, $M_{T2} = Tr_2$ stands for motor torque, $M_{f2} = F_{c2} + C_{s2}\omega_2$ stands for friction torque, ω_2 stands for the angular velocity of warp beam.

2.4. Disturbance Factors Modeling

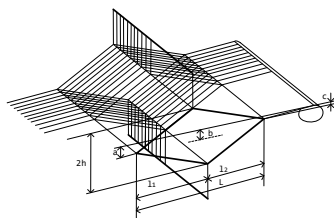


Figure 5. Schematic of heald frame mechanism

According to Figure 5, the yarn is stretched at the heald frame, so the influence of warp tension caused by heald frame is introduced.

The warp deformation at the heald frame is divided into upper and lower parts, and both are equal. According to the corresponding geometric relationship, we can get the warp length variables at the heald frame as follows:

$$\Delta L_1 = \Delta L_2 = \frac{h^2 - 2h(b-a)}{2l_1} + \frac{h^2 - 2h(b-c)}{2l_2} \quad (11)$$

According to the motion law of the heald frame as sinusoidal acceleration motion, the displacement of the heald frame in a motion cycle can be expressed as follow:

$$h = \begin{cases} 0.5H \sin^2 \omega_2 t & \omega_2 t \leq 90^\circ \text{ or } \omega_2 t \geq 270^\circ \\ 0.5H & 90^\circ < \omega_2 t < 270^\circ \end{cases} \quad (12)$$

Therefore, the maximum deformation caused by the movement of the heald frame to stretch the length of the warp yarn is as follow:

$$\Delta L = \Delta_1 + \Delta_2 = \frac{H^2}{4} \left(\frac{1}{l_1} + \frac{1}{l_2} \right) \sin^2 \omega_2 t \quad (13)$$

2.5. Tension Modeling

According to the above analysis, the yarn tension mathematical modeling can be obtained as follow:

$$\begin{cases} \dot{\omega}_1 = \frac{1}{J_1} (i_1 M_1 + Tr_1 - C_{s1} \omega_1 - F_{c1}) \\ \dot{\omega}_2 = \frac{1}{J_2} (i_2 M_2 - Tr_2 - C_{s2} \omega_2 - F_{c2}) \\ T = K_f \left(\int_{t_0}^t (\omega_2 r_2 - \omega_1 r_1) dt + \lambda \sin^2 \delta t \right) + B_f ((\omega_2 r_2 - \omega_1 r_1) + \lambda \delta \sin 2\delta t) \end{cases} \quad (14)$$

Then, the state space equation of the loom tension can be defined as follow:

$$\begin{cases} \dot{x}_t = \tilde{A}x_t + \tilde{B}u_t + d_t \\ y_t = \tilde{C}x_t \\ x_t = \Phi_t \end{cases} \quad (15)$$

where $\tilde{A} = \begin{bmatrix} a_{11} & a_{12} & a_{13} \\ a_{21} & a_{22} & 0 \\ a_{31} & 0 & a_{33} \end{bmatrix}$, $\tilde{B} = \begin{bmatrix} b_{11} & b_{12} \\ b_{21} & 0 \\ 0 & b_{32} \end{bmatrix}$, $\tilde{C} = \begin{bmatrix} 1 \\ 0 \\ 0 \end{bmatrix}^T$,

in which

$$a_{11} = -B_f \left(\frac{r_1^2}{J_1} + \frac{r_2^2}{J_2} \right), \quad a_{12} = \frac{C_{s1}}{J_1} B_f r_1 - K_f r_1, \quad a_{13} = K_f r_2 - \frac{C_{s2}}{J_2} B_f r_2, \quad a_{21} = \frac{r_1}{J_1}, \quad a_{22} = -\frac{C_{s1}}{J_1},$$

$$a_{31} = -\frac{r_2}{J_2}, \quad a_{33} = -\frac{C_{s2}}{J_2}, \quad b_{11} = -\frac{i_1}{J_1} B_f r, \quad b_{12} = \frac{i_2}{J_2} B_f r_2, \quad b_{21} = \frac{i_1}{J_1}, \quad b_{32} = \frac{i_2}{J_2}.$$

$$d_t = \begin{bmatrix} K_f \lambda \delta \sin 2\delta t + B_f \lambda \delta^2 \sin 4\delta t + \frac{F_{c1}}{J_1} B_f r_1 - \frac{F_{c2}}{J_2} B_f r_2 \\ -\frac{F_{c1}}{J_1} \\ -\frac{F_{c2}}{J_2} \end{bmatrix} \text{ is the internal disturbance factors in the}$$

system, and the total disturbance of the system is set as $\tilde{B}f(x_t) = d_t + d_{tt}$ in which d_{tt} is the external disturbance factors in the system, ϕ is the initial state of the system.

Then, Equation (16) can be obtained as follow by discretizing Equation (15):

$$\begin{cases} x_{k+1} &= Ax_k + B(u_k + f(x_k)) \\ y_k &= Cx_k \\ x_k &= \phi_k \end{cases} \tag{16}$$

in which $A = e^{\tilde{A}T}$, $B = \int_0^T e^{As} ds$, $C = \tilde{C}$.

3. Networked Control System Modeling

Considering the following uncertain nonlinear time-invariant discrete-time system with time delay:

$$\begin{cases} x_{k+1} &= (A + \Delta A)x_k + A_d x_{k-\tau_k} + B(u_k + f(x_k)) \\ y_k &= Cx_k \\ x_k &= \phi_k \end{cases} \tag{17}$$

in which $x_k \in \mathbb{R}^n$, $u_k \in \mathbb{R}^m$ and $y_k \in \mathbb{R}^p$ are the system state, system input, and system output measurement, respectively. The matrices A , A_d , B and C are known constant matrices with proper dimensions, $x_{k-\tau_k}$ stands for the time delay, $f(x_k)$ is the disturbance vector which belonging to $l_2[0, \infty)$.

Assumption 1: ΔA is a norm-bounded parameter-uncertainty matrix and can be described as:

$$\Delta A = EFH \tag{18}$$

in which F is an unknown matrix which satisfies $FF^T \leq I$, E and H are known constant matrices with proper dimensions.

Assumption 2: The nonlinear disturbance $f(x_k)$ is bounded and satisfies:

$$\|f(x_k)\| \leq \lambda \|x_k\| \tag{19}$$

with $\lambda > 0$ stands for a known scalar.

Assumption 3: The system is fully controllable and observable, in other words, (A, B) and (A, C) are full rank.

3.1. Quantization

In the networked control system, information transmission between components is carried out through communication channels. For information to be transmitted in the channel, it must first be quantized and encoded. Meanwhile, considering that the bandwidth of the channel is limited

in practical applications, to ensure that the system can operate normally within a given bandwidth, it is necessary to use the quantization technique to reduce the communication rate.

The logarithmic quantizer which applied in this paper can be described as follow:

$$Q(\hat{u}) = [Q_1(\hat{u}_1) \ Q_2(\hat{u}_2) \ \cdots \ Q_m(\hat{u}_m)]^T \tag{20}$$

in which $\hat{u}_i, i = 1, 2, \dots, m$, is the i th element in the \hat{u} and satisfied $Q_i(-\hat{u}_i) = -Q_i(\hat{u}_i)$.

The values of $Q_i(\hat{u}_i)$ in $Q(\hat{u})$ can be described as:

$$Q_i(\hat{u}_i) = \begin{cases} u_i^j \text{sign}(u_i), & \frac{u_i^j}{1+\delta_0} \leq |u_i| \leq \frac{u_i^j}{1-\delta_0} \\ 0, & |u_i| < \frac{u_{min}}{1+\delta_0} \end{cases} \tag{21}$$

in which $u_i^j = \rho_0^{1-j} u_{min}, i = 1, 2, \dots, \rho_0 = 1 - \delta_0 / 1 + \delta_0, \delta_0 \in (0, 1)$, where u_{min} is the quantified dead zone, ρ_0 is the quantified density, j can be seen as the quantified level. Define quantified error $\Delta_k(\hat{u}_k) = Q(\hat{u}_k) - \hat{u}_k$ with $\Delta_k = \text{diag}\{\Delta_k^1, \Delta_k^2, \dots, \Delta_k^m\}$ and $\|\Delta_k^i\| \leq \delta_i, i \in \{1, 2, \dots, m\}$, then, we can obtain that

$$Q(\hat{u}_k) = (I + \Delta_k)\hat{u}_k \tag{22}$$

3.2. Packet Loss

Due to the instability of the network, data packets may be lost during transmission. To compensate data packet loss, following method is proposed:

$$y_k = \begin{cases} y_k, & \text{when data packets are received;} \\ y_{k-1}, & \text{when data packets are lost.} \end{cases} \tag{23}$$

Equation (23) stands for $y_k = y_k$ when data packets are received at time k , and $y_k = y_{k-1}$ when not. The possibility of the occurrence of packet loss can be described as a Bernoulli distribution as follow:

$$\begin{cases} P(\theta_k = 1) & = \theta \\ P(\theta_k = 0) & = 1 - \theta \end{cases} \tag{24}$$

in which $0 \leq \theta \leq 1$ and $\theta_k = 1$ stands for occurring packet loss, $\theta_k = 0$ stands for not. Then Equation (23) can be rewritten as follow:

$$y_k = \theta y_k + (1 - \theta) y_{k-1} \tag{25}$$

Substitute Equation (22) and Equation (25) into Equation (17), the control model of the networked system with quantification, delay and packet loss can be obtained as follow:

$$\begin{cases} x_{k+1} & = (A + \Delta A)x_k + A_d x_{k-d_k} + B((I + \Delta_k)\hat{u}_k + f(x_k)) \\ y_k & = \theta y_k + (1 - \theta) y_{k-1} \end{cases} \tag{26}$$

3.3. Event-triggered Scheme

An event-triggered scheme is applied in this paper to minimize system bandwidth occupancy and increase the component serving life in the tension control system. Only when the event-triggered condition stated in Equation (27) is fulfilled, the data from the sensor will be sent to the controller.

$$e_{\hat{x}_k}^T \Omega e_{\hat{x}_k} \geq \delta \hat{x}_k^T \Omega \hat{x}_k \tag{27}$$

where $\delta \in [0,1]$ is a constant, $e_{\hat{x}_k} = \hat{x}_k - \hat{x}_{k-}$ in which \hat{x}_k and \hat{x}_{k-} are the current measurement and the system state at the last moment, respectively. $\Omega > 0$ is the weighting matrix and is known.

4. Main Results

This section establishes an event-triggered sliding mode control scheme for the networked control system under consideration. The state trajectories are forced onto the pre-designed sliding surface by the observed-based sliding mode controller. Figure 6 depicts a complete flowchart.

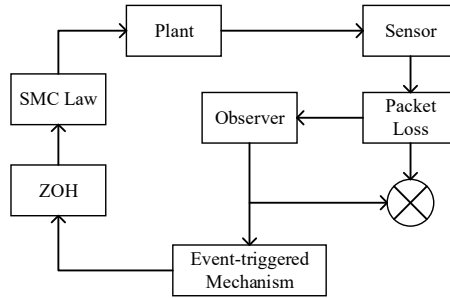


Figure 6. The detailed flowchart of control system

4.1. Observer Design

According to reference [12], the following state observer is proposed:

$$\hat{x}_{k+1} = A\hat{x}_k + Bu_k(I + \Delta_k) + L[y_k - (1 - \theta)C\hat{x}_k] \quad (28)$$

where $\hat{x}_k \in \mathbb{R}^n$ is the observed value of the system state and $L \in \mathbb{R}^{n \times p}$ is the observer gain value to be designed later.

The sliding surface is selected as follow:

$$S_k = G\hat{x}_k \quad (29)$$

in which matrix $G \in \mathbb{R}^{m \times n}$ needs to ensure $GB(I + \Delta)$ is non-singular and will be designed later.

An ideal sliding surface should satisfy the following condition:

$$S_k = S_{k+1} = 0 \quad (30)$$

The equivalent control of the system may be accomplished as follows when the system state reaches the ideal sliding surface according to Equation (28)-(30):

$$u_{eq}^k = -(GB(I + \Delta_k))^{-1}G[A\hat{x}_k + L(y_k - (1 - \theta)C\hat{x}_k)] \quad (31)$$

Substituting the Equation (27) into Equation (31), and then we can obtain that:

$$u_{eq}^k = -(GB(I + \Delta_k))^{-1}G[A\hat{x}_{k-} + L(y_k - (1 - \theta)C\hat{x}_{k-})] \quad (32)$$

Substituting Equation (32) into Equation (28), the sliding surface of the system can be obtained as follow:

$$\begin{aligned} \hat{x}_{k+1} = & [A - (\theta_k - \theta)LC](I - \bar{G})\hat{x}_k + \bar{G}Ae_{\hat{x}_k} + (1 - \theta_k)(I - \bar{G})L Ce_k + \\ & \theta_k(I - \bar{G})L Ce_{k-1} + \theta_k(I - \bar{G})L C\hat{x}_{k-1} \end{aligned} \quad (33)$$

where $\bar{G} = B(I + \Delta_k)(GB(I + \Delta_k))^{-1}G$, and the error dynamic can obtain as follow:

$$\begin{aligned} e_{k+1} = & (A + \Delta A - (1 - \theta_k)LC)e_k + A_d e_{k-\tau_k} + B(I + \Delta_k)f(x_k) - \theta_k L Ce_{k-1} - \theta_k L C\hat{x}_{k-1} + \\ & (\Delta A + (\theta_k - \theta)LC)\hat{x}_k + A_d \hat{x}_{k-\tau_k} \end{aligned} \quad (34)$$

4.2. Observed-based SM Controller Design

The sliding mode control law is proposed in this section to reduce the effect of the event-triggered mechanism and the network factors, allowing the system state to approach the pre-designed sliding surface in a limited time.

Theorem 1: For state observer Equation (28) and sliding surface Equation (29), if

$$u_k = -(GB(h, r_k))^{-1}[GA\hat{x}_{\bar{k}} + GL(y_k - (1-\bar{\theta})\hat{y}_k) - \Lambda \text{sgn}(S_{\bar{k}})] \quad (35)$$

with $\Lambda \begin{cases} > \|GA\| \|e_{\hat{x}_k}\| + \rho, & \text{if } S_k^T \text{sgn}(S_{\bar{k}}) > 0 \\ \leq \|GA\| \|e_{\hat{x}_k}\| + \rho, & \text{otherwise} \end{cases}$ where $\rho > 0$ is a constant, then the system state can approach the pre-designed sliding surface in a limited time.

Proof:

Define the following Lyapunov-Krasovskii function:

$$V_k = \frac{1}{2} S_k^T S_k \quad (36)$$

and its increment

$$\begin{aligned} \mathbb{E}\{\Delta V_k\} &= \mathbb{E}\{V_{k+1}\} - \mathbb{E}\{V_k\} \\ &= \frac{1}{2} S_{k+1}^T S_{k+1} - \frac{1}{2} S_k^T S_k \\ &= \frac{1}{2} S_{k+1}^T S_{k+1} - \frac{1}{2} S_k^T S_k + S_k^T S_{k+1} - S_k^T S_{k+1} \\ &= S_k^T \Delta S_k + \frac{1}{2} S_{k+1}^T \Delta S_k^T - \frac{1}{2} S_k^T \Delta S_k^T \\ &= S_k^T \Delta S_k + \frac{1}{2} \Delta S_k^T \Delta S_k \\ &= S_k^T S_{k+1} - S_k^T S_k + \frac{1}{2} \Delta S_k^T \Delta S_k \end{aligned} \quad (37)$$

in which $\Delta S_k = S_{k+1} - S_k$.

By substituting Equation (35) into Equation (29) can obtain that:

$$S_{k+1} = -GAe_{\hat{x}_k} - \Lambda \text{sgn}(S_k^-) \quad (38)$$

Meanwhile, considering $\|S_k\| \leq \|S_k\|_1$, then we have:

$$\mathbb{E}\{\Delta V_k\} \leq -\rho \|S_k\| - S_k^T S_k + \frac{1}{2} \Delta S_k^T \Delta S_k \quad (39)$$

Then from above all, we can ensure $S_k = 0$ by adjusting the positive parameter ρ to make ΔV_k^6 is negative and ΔS_k is reasonably bounded which also implies the proof is complete.

5. An Illustrative Example

The initial conditions of the loom tension control system and state observer are set as $x_0 = [185 \ 300 \ 180]^T$, $\hat{x}_0 = [185 \ 115 \ 225]^T$, respectively and system parameter matrix are

$$\text{set as } A = \begin{bmatrix} -3.049 & 5.484 & 26.842 \\ -0.367 & 0 & 0.824 \\ 0 & -0.750 & 2.471 \end{bmatrix}, B = \begin{bmatrix} 13.180 & 0 \\ 0 & 7.908 \\ -69.271 & 155.862 \end{bmatrix}, C = \begin{bmatrix} 1 \\ 0 \\ 0 \end{bmatrix}^T, E = \begin{bmatrix} 26.842 \\ 23.897 \\ 0.824 \end{bmatrix},$$

$$H = \begin{bmatrix} 26.842 \\ 23.897 \\ 2.471 \end{bmatrix}^T, F(k) = \sin(k). \text{ Considering the variation range of delay as } \tau_m = 1 \text{ ms and}$$

$\tau_M = 3 \text{ ms}$, the total packet loss probability $\bar{\theta} = 0.2$, and the quantization parameter $\delta_0 = 0.1$, the quantizer density is set as $\rho_0 = 0.82$.

The simulation results are shown as follow. The closed-loop system states are asymptotically stable, and control signals tend to stabilize under the effects of time delay, packet losses, and data quantization, as shown in Figure 7 and Figure 8. The sliding variables tend to zero with time, as seen in Figure 9.

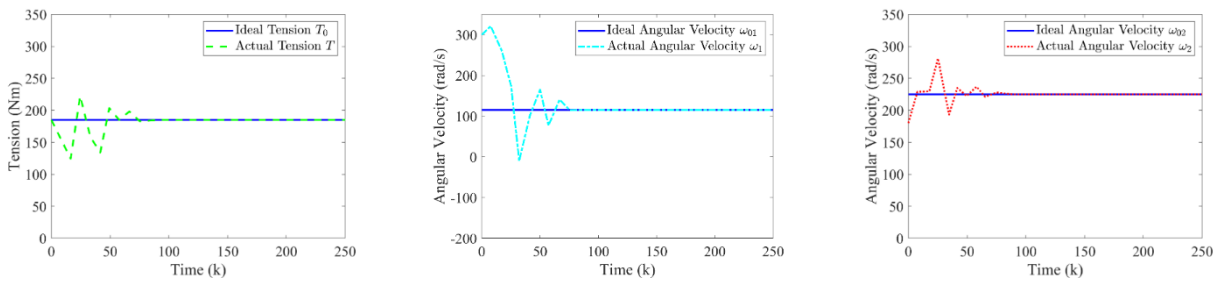


Figure 7. State trajectories of the system

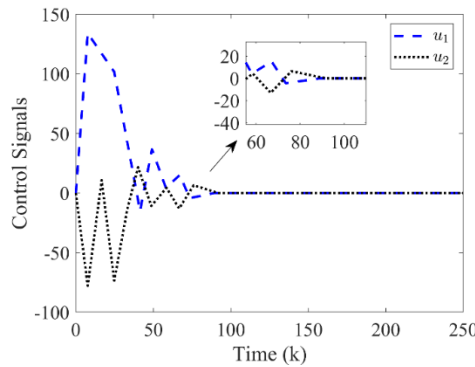


Figure 8. Control signals

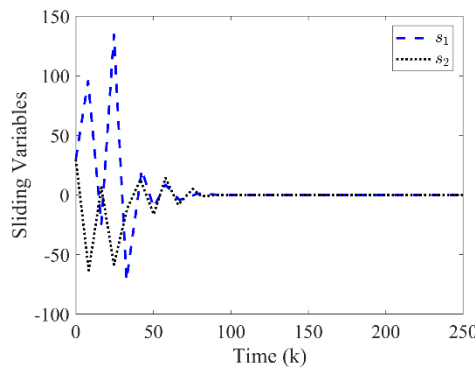


Figure 9. Sliding variables

6. Conclusion

In this paper, an observed-based sliding mode networked control with event-triggered scheme is proposed. By introducing the networked control method to the tension control of the carbon fiber diagonal loom, we established its networked model includes time delay, quantization, and packet loss. Then, a novel sliding surface and a sliding mode control law have been synthesized to ensure the asymptotic stability of the system. Finally, the simulation results show that the proposed control algorithm can realize rapid convergence of the tension system. In the future work, we shall be devoted to find more control methods to increase the stability of loom tension control under unexpected disturbances.

References

- [1] Chocron, Sidney, et al: Impact on carbon fiber composite: Ballistic tests, material tests, and computer simulations, *International Journal of Impact Engineering* 131 (2019), p.39-56.
- [2] Kim, H. K., et al: A study on correlation between warp tension and weaving condition, *Fibers and Polymers* 14(2014) No.12, p.2185-2190.
- [3] Xiao, Y., et al: Optimal analysis and application of the warp tension control system for a rapier loom, *Textile Research Journal* 92(2021), p.1213-1225.
- [4] Xu, G., et al: The Equivalent Sliding Mode Tension Control of Carbon Fiber Multilayer Diagonal Loom, *International Journal of Control, Automation and Systems* 17(2019), No. 7, p.1762-1769.
- [5] Liu, W., et al: Discrete Global Sliding Mode Control for Time-Delay Carbon Fiber Multilayer Diagonal Loom, *IEEE Access* 5(2017), p.15326-15331.
- [6] Xiao, Y., et al.: Research and Embedded Implementation of Let-Off and Take-Up Dynamic Control Based on Fuzzy Neural Network and Vector Control Optimization, *IEEE Access* 10(2022), p.17768-17780.
- [7] Xiao, Y., et al: Research on integral separation control of warp tension based on fuzzy parameter optimization, *Journal of Intelligent & Fuzzy Systems* 41(2022), No. 2, p.3031-3044.
- [8] Karnoub, A., et al: Using the expert system to analyze loom performance, *The Journal of The Textile Institute* (2016), p.1-13.
- [9] Mahmoud, M. S. and M. M. Hamdan: Fundamental issues in networked control systems, *IEEE/CAA Journal of Automatica Sinica* 5(2018), No. 5, p.902-922.
- [10] Wang, X., et al: Dynamic Friction Parameter Identification Method with LuGre Model for Direct-Drive Rotary Torque Motor, *Mathematical Problems in Engineering* (2016), p.1-8.
- [11] Zhang, M., et al: Network-based fuzzy control for nonlinear Markov jump systems subject to quantization and dropout compensation, *Fuzzy Sets and Systems* 371(2019), p.96-109.
- [12] Guan, X., et al: Observer-based sliding mode control for discrete nonlinear systems with packet losses: an event-triggered method, *Systems Science & Control Engineering* (2020), No. 1, p.175-188.